SCALING LAW APPLICABLE TO DESIGN OF MPD ARCJET

Yukio Shimizu*
Institute of Space and Astronautical Science,
3-1-1, Yoshinodai, Sagamihara, Kanagawa 229-8510, Japan
Kyoichi Kuriki**
Tokyo Metropolitan Institute of Technology
6-6, Asahigaoka, Hino-shi, Tokyo 191-0065, Japan

Abstract

A simple model for the discharge region of an MPD arcjet is analyzed to find its design guideline. Concentric cathode and anode surfaces constitute the end surface of semi-infinite space, where the discharge current freely flows axially and radially. By applying the principle of minimum work, extension of the discharge region is obtained. Dependence of the derived extension on input power gives a scaling law useful for the MPD arcjet design.

Nomenclature

A	discharge shape factor
$\overline{A}$	mean distance of electrodes
a	diameter of cathode
B	self-induced field
B_ϑ	azimuthal magnetic density
b	inner diameter of anode
b_Z	non-dimensional factor
c	radial distance
dx	depth of plasma
e	expansion force
F	thrust
f	blowing force
g	Joule heating
h	pinch force
J	total current
J	discharge current
j	current density
j_r	radial current
j_x	axial current
ℓ	axial distance
$\dot{m}$	mass flow rate
P	discharge power
P_h	heat power
P_i	ionization power
P_j	Joule power
P_{loss}	power loss
P_a	acceralation power
R	magnetic Reynolds number
r_a	anode radius
r_c	cathode radius
V	discharge voltage
δ	non-dimensional number
ϕ	work function
σ	electric transaction
η	efficiency
η_e	efficiency with compression
ρ	density
μ	magnetic factor
ξ	non-dimensional number

* Engineer, Member JSASS, AIAA,
** Professor, Member JSASS, Fellow AIAA,

Introduction

The pulsed MPD arcjet system, EPEX (Electric Propulsion Experiment) was flight-tested onboard the SFU (Space Flyer Unit). The SFU was launched in 1995 and the EPEX system was validated for the planned propulsive functions [Ref. 1, 2]. The discharge chamber of EPEX MPD arcjet has configuration depicted in Fig. 1. Design of the chamber is based on the experimental results such as [Ref. 3]

1) Short cathode and cone-shaped nozzle of electrical insulator are effective in enhancing both electrothermal and electromagnetic thrust generation,
2) Arc discharge is rather limited in the upstreamregion,

These features are taken into account without in-depth analytical considerations.

The MHD analyses which had been done until late 1980's are mostly focused on quasi-one-dimensional

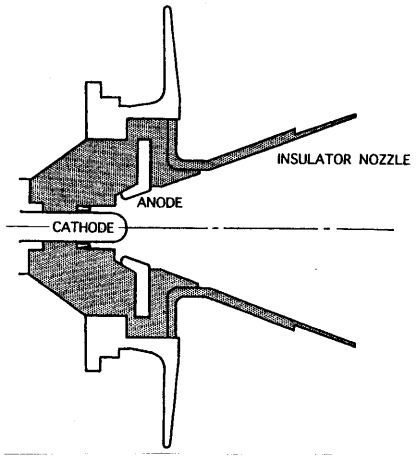

Fig. 1 The discharge chamber of EPEX/MPD arcjet

channel flow, namely the flow in the annular region between rod cathode and cylindrical anode[Ref.4]. Although the one-dimensional flow analyses are developed with reference to the channel length L, results of thrust or specific impulse thus obtained are not given as explicit function of the size L, as is well known from the electromagnetic acceleration. From experimental results, however, the discharge region is not confined in the annular channel, but extends into free space outside the channel especially when the molecular gases like H_2 and N_2 are used as propellant [Ref. 5]. The dimension of discharge region, therefore, should be determined by taking into account the discharge behavior outside the channel. Some numerical studies were done for such flows, but still insufficient to provide parametric dependence of discharge extension, above all the dependence on the input power [Ref. 6]. As for EPEX/MPD arcjet the electrodes are essentially short and far from the one-dimensional channel. Moreover, since the propellant is mixture of H_2 and N_2 simulating N_2H_4, the arc discharge extends downstream.

Considering the realities mentioned above, analyzed in the present studies are the extensions of discharge and acceleration region in the semi-infinite free space intentionally eliminating the annular channel. The discharge power P as well as the discharge voltage V should be dependenct upon discharge current J, mass flow rate $\dot{m}$, radius of cathode disk a, and radius of anode ring, b.

The discharge voltage should be determined self-consistently from the power required for the discharge and acceleration. For the calculation of power it is essential to specify the border dimension of discharge region c, which even in the case of computational fluid dynamics is frequently assumed a priori. In the present analysis as well be shown later such dimension is made free and duly determined by applying "Minimum Work Principle" to the total discharge power. By taking variation with respect to the dimension c macroscopic consistency is more stressed than the local details.

The purposes of the present analysis are to

1) Give analytical background to the experimentally determined EPEX/MPD arcjet design, and

more generally for given input power to clarify

2) Whether the arcjet size should be determined from MHD behavior and discharge pattern, or thermal loading on the arcjet structure

as the design guideline.

Analytical Model

The model used for the present analysis is shown in Fig. 2. The left hand side $x < 0$ is occupied by a rod cathode, a concentric annular anode, and an insulator separating the two electrodes. The typical flow pattern of the discharge current is sketched in Fig. 2 as observed experimentally. The plasma expands hemispherically and the current paths close within the radial and axial distances, c and ℓ, respectively. The radial and axial currents, j_r and j_x interact with the azimuthal self-induced field B , generating blowing, pinch and expansion forces. The blowing force directly serves as thrust and the pinch force indirectly contributes to the thrust generation by enhancing the plasma pressure near the centerline.

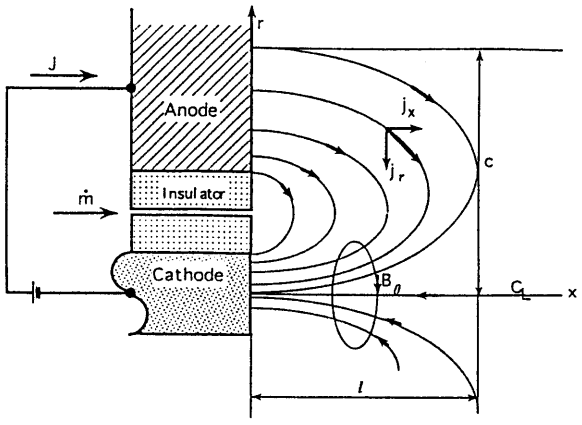

Fig. 2 The discharge current flow pattern.

The experimental observation does not show any definite outward boundaries like c and ℓ, but these dimensions represent typical spread of plasma, which enable us to derive simple expression of the scaling law. In the present analysis the hemispherical plasma is

approximated by the cylindrical one as shown in Fig. 3. The discharge current starting from the anode surface at r = r_1 flows in the x-direction until it reaches the conical surface connecting the circles (0, b) and (ℓ, c). Thereafter changing the flow direction by 90 degrees, the current flows radially inward to the virtual cathode of radius a, which is so-called cathode jet. The radially inward current is assumed to have uniform distribution in the x-direction. The fraction of total current J flowing radially in the disk of thickness dx is Jdx/ℓ. The density of axial current $j_x(r_1)$ flowing in the cylindrical shell of radius r_1, length x and thickness dr_1 as sketched in Fig. 3 is obtained from the equation

$$2\pi r_1 j_x(r_1)dr_1 = jdx / l \qquad (1)$$

The conical surface extending between (0, b) and (ℓ, c) is expressed as

$$r_1 = b + (c-b)x / l \qquad (2)$$

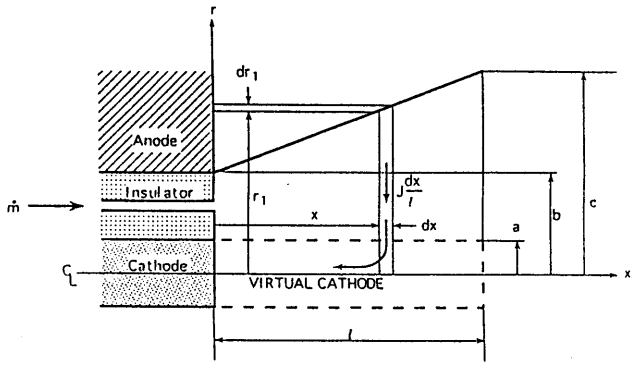

Fig. 3 Simplized discharge current flow pattern.

The virtual cathode located in $r \le a$ corresponds to the well-known cathode jet in which the plasma is compressed to have high temperature. The current flowing upstream in this region is assumed to have a uniform radial distribution. For the calculation of the Joule heating the electrical conductivity σ is assumed to be constant all over the region considered. To summarize the domain of analysis consists of the three regions, **I**, **II** and **III** as shown in Fig. 4. The types of power deposited are,

Joule heating : region **I**, **II** and **III**,

Pinching power : region **I**,

Blowing power : region **II**,

Expansion power : region **III**,

in the respective regions.

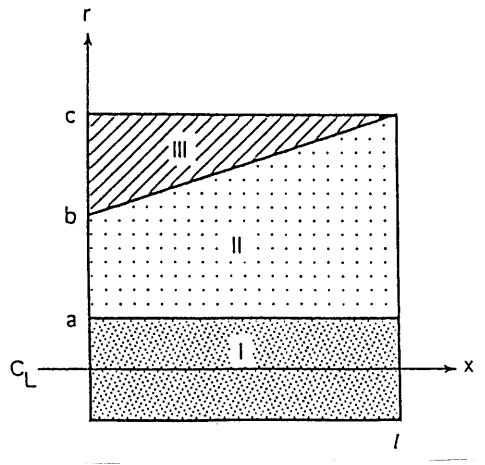

Fig. 4 The domain of analysis regions.

If the full numerical solution were to be found for the present problem, the line integration of electric strength along any field line from cathode to anode should be found same. Relying on the variational principle, the consistency of local details as such may be lost. However in the present analysis "Minimum Power Principle" is applied to the total power as macroscopic process to find the typical dimension of the discharge region. For a given discharge current the determination of input power in such a manner should be nothing but obtaining the discharge voltage. For the question how we can validate the present scheme, the agreement with the experimental results can be asserted. Once the agreement is confirmed, the present scheme offers greater convenience by showing parametric dependence on operational conditions.

Electromagnetic Forces

Pumping Force

Pumping force is generated in the region **I**. The plasma compressed towards centerline eventually obtains axial momentum, thereby generating the thrust.

The azimuthal magnetic field Bt in the region **I** is given by the equation,

$$B_\theta = \frac{\mu J_a}{2\pi r} \qquad (3)$$

where J_a is the total current flowing within the circuit of radius r. The density of axial current j_x is assumed to be uniform over the cross section.

$$j_x = \frac{J}{\pi a^2}\left(1 - \frac{x}{l}\right) \qquad (4)$$

Multiplying the circle area πr^2, one can obtain the current J_a.

$$J_a = \frac{Jr^2}{a^2}(1-\frac{x}{l}) \qquad (5)$$

Inserting J_a into Eq.(3), one can find B_ϑ,

$$B_\vartheta = \frac{\mu Jr}{2\pi a^2}(1-\frac{x}{l}) \qquad (6)$$

The Lorentz force is calculated multiplying B by j_x in Eq.(4). The pumping force results from the integration of the Lorentz force over the whole volume of region **I**.

$$H = \int_0^l \int_0^a j_x B_\vartheta \cdot 2\pi r\, dr\, dx = \frac{\mu J^2 l}{9\pi a} \qquad (7)$$

The power required for the pumping work depends on the local mass flow of which the distribution is out of scope in the present analysis. For simplicity, the mass flow rate related with the pumping work is assumed to be the total mass flow rate $\dot{m}$. The required power is therefore $H^2/2\dot{m}$.

Blowing Force

The blowing force is generated in the region **II** in Fig. 4. The force is axial and directly contributes to the thrust generation. The current distribution in Fig. 3 is referred to for the blowing force calculation. The azimuthal magnetic field in this region is given by the equation

$$B_\vartheta = \frac{\mu J}{2\pi r}\left(1-\frac{x}{l}\right), \qquad (8)$$

The current density has only radial component j_r.

$$j_r = \frac{J}{2\pi r l} \qquad (9)$$

The total blowing force is obtained by integrating the Lorentz force over the region **II**.

$$F = \int_0^l \int_0^{r_1} j_x B_\vartheta\, 2\pi r\, dr\, dx$$

$$= \frac{\mu J^2}{4\pi a}\left\{\ln\left(\frac{b}{a}\right)+\left(\frac{b}{c-a}\right)^2 \ln\left(\frac{c}{b}\right)-\frac{3c-b}{2(c-b)}\right\} \qquad (10)$$

In the limit $c \to b$, we find

$$F \to \frac{\mu J^2}{4\pi}\ln\left(\frac{b}{a}\right), \qquad (11)$$

the well known thrust formula (Ref. 7). When the mass flow rate is assumed same as that for the pumping force, i.e. $\dot{m}$, the power required for the blowing work is $F^2/2\dot{m}$.

Expansion Force

The expansion force is obtained by calculating the radial electromagnetic force in the cylindrical shell of radius r_1, length x and radial thickness dr_1 in Fig. 3. The axial current density j_r in the region **III** is obtained from current continuity equation, Eq. (1). The azimuthal magnetic field is found same as the one in Eq. (3). The total expansion force is the integration,

$$E = \int_b^c j_x B_\vartheta 2\pi r_1\, x\, dr_1, \qquad (12)$$

which, r_1 being the function of x, is converted into x-wise integration using the relation Eq. (2). The result is

$$E = \frac{\mu J^2 l}{2\pi}\left\{\frac{c+b}{2(c-b)^2}-\frac{bc}{(c-b)^3}\ln\left(\frac{c}{b}\right)\right\} \qquad (13)$$

Similarly to the former two forces the power required for the expansion work is $E^2/2\dot{m}$.

Joule Heating

The input power dissipated as Joule heating is obtained by integrating the density j^2/σ over the three regions **I** through **III**.

Region **I** $(r \le a)$

The current density $j=j_x$ is given by Eq. (4). The power

dissipated in this region is the straightforward integration,

$$P_j(I) = \frac{1}{\sigma}\int_0^l j_x \pi a^2 dx$$

$$= J^2 l / 2\pi\sigma a^2 \qquad (14)$$

Region **II** $(a \le r \le r_1)$

The current density j_r is given by Eq. (9). The power dissipated in this region results as follows.

$$P_j(II) = \frac{1}{\sigma}\int_0^l \int_a^{r_1} j r^2 2\pi r dr dx$$

$$= \frac{J^2}{2\pi\sigma l}\left\{\ln\left(\frac{b}{a}\right) - 1 + \frac{c}{c-b}\ln\left(\frac{c}{b}\right)\right\} \qquad (15)$$

Region **III** $(r_1 \le a \le c)$

Likewise in the former two regions, the Joule heating power is calculated by using the current density j_x in Eq. (1).

$$P_j(III) = \frac{1}{\sigma}\int_l^c j x^2 2\pi r_1 dr_1$$

$$= \frac{J^2}{2\pi\sigma}\left\{\frac{1}{(c-b)^2} - \frac{b}{(c-b)^3}\ln\left(\frac{c}{b}\right)\right\} \qquad (16)$$

Total Power

The total power P for electromagnetic work and Joule heating is obtained by adding the foregoing powers altogether.

$$P = \frac{1}{2\dot{m}}(H^2 + F^2 + E^2) + G \quad , \qquad (17)$$

where $G = P_j(I) + P_j(II) + P_j(III)$. The power P as well as its components, H, F, E and G are normalized by the representative power $J^2 / \pi\sigma b$ as follows.

$$p(z;A,R) = \frac{R}{8}\left\{h^2(z;A) + f^2(z;A) + e^2(z)\right\} + g(z;A) \quad , \qquad (18)$$

where

$$h(z;A) = 4Az / 9 \ ,$$

$$f(z;A) = \ln A + \left(\frac{z}{z-1}\right)^2 \ln z - \frac{3z-1}{2(z-1)} \ ,$$

$$e(z) = \frac{z(z+1)}{(z-1)^2} - \frac{2z^2}{(z-1)^3}\ln z \ ,$$

$$g = \frac{A^2}{3}z + \frac{1}{2z}\ln A + \frac{1}{2(z-1)}\ln z - \frac{1}{2z} + \frac{z}{2(z-1)^2} - \frac{z}{2(z-1)^3}\ln z \ ,$$

$$R = \sigma\mu b\left(\mu J^2 / 4\pi\dot{m}\right), \quad A = a / b \qquad (19)$$

In the above expression we assumed ℓ=c and used the expression z=c/b=ℓ/b. The parameter R is magnetic Reynolds number consisting of representative velocity $\mu J^2 / 4\pi\dot{m}$ and the length b.

Numerical Results

The functions in Eq. (19), h(z; A), f(z; A), e(z) and g(z; A) are calculated and shown in Figs. 5 through 8 changing the parameter A. These results indicate that the functions h(z; A), f(z; A), e(z) are monotonously increasing functions of z and only g(z; A) has a minimum. Comparing the absolute values of the four functions, we find g(z; A) is dominant in p(z; A, R) which is shown in Fig. 9. Therefore, when we apply "Minimum Work Principle" to p(z; A, R) by differentiating with respective to z, the results are strongly dependent on the behavior of g(z; A). When z = c/b decreases to unity, the region **III** becomes infinitely thin cylindrical shell as observed in Fig. 4 and the Joule dissipation, i.e. g(z; A) becomes infinitely large. As z increases, on the other hand, the Joule dissipation decreases in the region **III**, but increases in the region **I** since we assume c = ℓ and z = ℓ/b. With these effects combined the minimum work results from the variational principle.

The non-dimensional dimension of discharge region $z=(c/b)_{min}$ determined by the process above is shown in Fig. 10. The dimension $(c/b)_{min}$ is found weakly dependent on A = a/b and the magnetic Reynolds number in the practical range of these parameters. The thrust

efficiency η

$$\eta = Rf^2(z;a) / 8p(z;A,R) \qquad (20)$$

is dependent only on the blowing force and its values at $(c/b)_{min}$ are shown in Fig. 11. For the weak dependence of $(c/b)_{min}$ on R, η is almost linearly proportional to R as expected from Eq. (20).

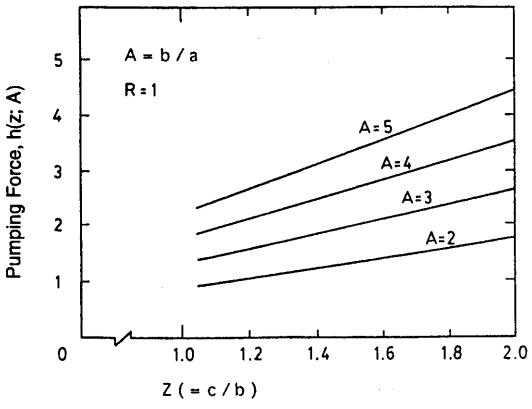

Fig. 5 Numerical results of h(z;A).

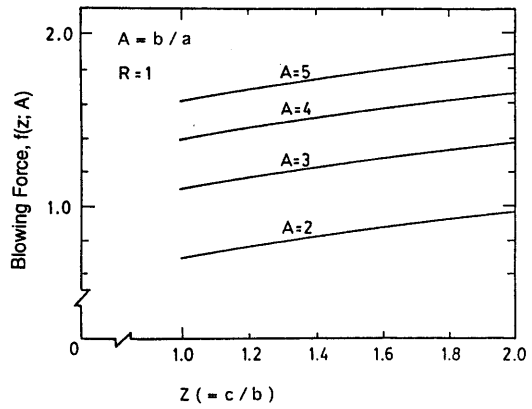

Fig. 6 Numerical results of f(z;A).

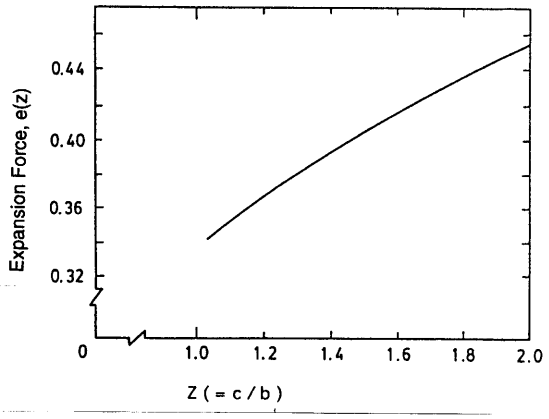

Fig. 7 Numerical results of e(z).

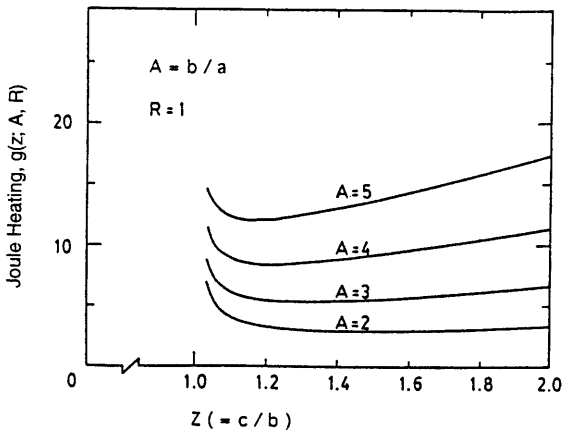

Fig. 8 Numerical results of g(z;A).

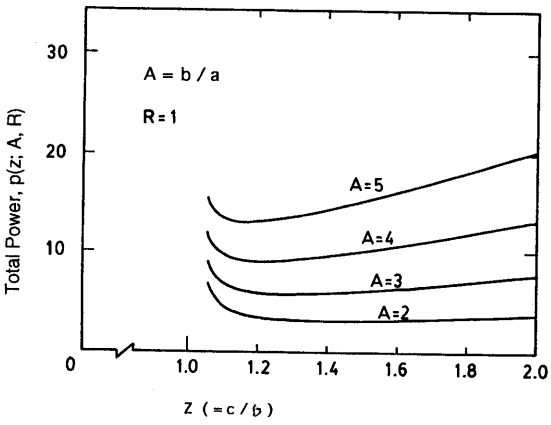

Fig. 9 Numerical results of p(z; A,R).

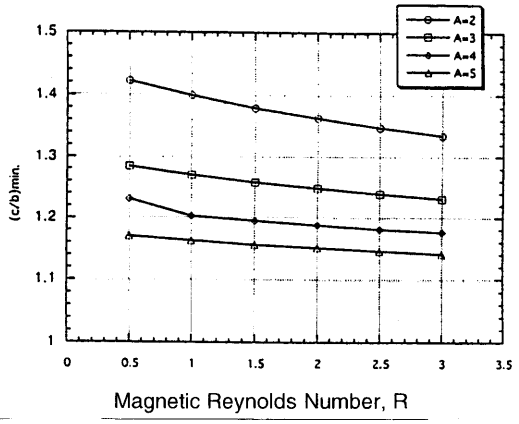

Fig. 10 Numerical results of dimension z vs R.

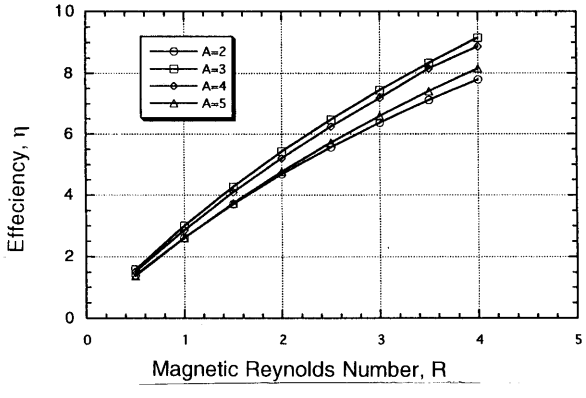

Fig. 11 Numerical results of η vs R.

Discussion

As explained earlier, the present analysis has been motivated by determining the electrode dimensions in designing the MPD arcjet of EPEX flown aboard SFU. The configuration of the discharge chamber shown in Fig. 1 has been based on the experimental experiences that the flare anode and the short cathode are favorable to the thrust performance. The shorter flare anode attached with insulator nozzle was found best and explained in terms of "reverse pinch" effect (Ref. 3). The insulator nozzle is also effective in generating electrothermal thrust in the range of specific impulse 1,000 – 1,500 s.

As far as the electrode dimensions are concerned, A=2 case in the present analysis corresponds to the model of EPEX/MPD arcjet. The $(c/b)_{min}$ = 1.40 or $(c/a)_{min}$ = 2.80 is obtained for A=2, showing reasonable agreement with experiment that about 75% of the discharge region exists in c/a < 4.0 as shown in Fig. 11 (Ref. 8). The agreement justifies the design of EPEX/MPD arcjet.

The "reverse pinch" mentioned above implies that the momentum of radial expansion is once converted into the wall pressure on the nozzle, and thereafter into the axial momentum, i.e. the thrust. Taking such effect into account, the thrust efficiency can be expressed by the following equation.

$$\eta_e = \frac{R\left\{f^2(z;A)+h^2(z;A)+e^2(z)\right\}}{8p(z;A,R)} \tag{21}$$

Comparing η_e in Fig.12 with η in Fig.13, improvements more than 20% are recognized and support effectiveness of the insulator nozzle. For the operational condition of EPEX model R $\cong$ 1, the measured thrust efficiency is about 30% and greater than the corresponding value of η_e. Since only the electromagnetic thrust is taken in account here, the electrothermal thrust is considered to additionally contribute to the thrust efficiency. As also found in Fig. 5 and 7, the axial pinch force h(z; A) is larger than the expansion force e(z) and provides greater contribution to η_e.

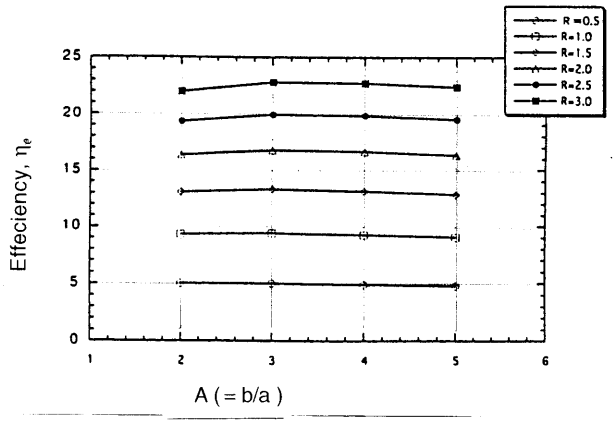

Fig. 12 Numerical results of η_e.

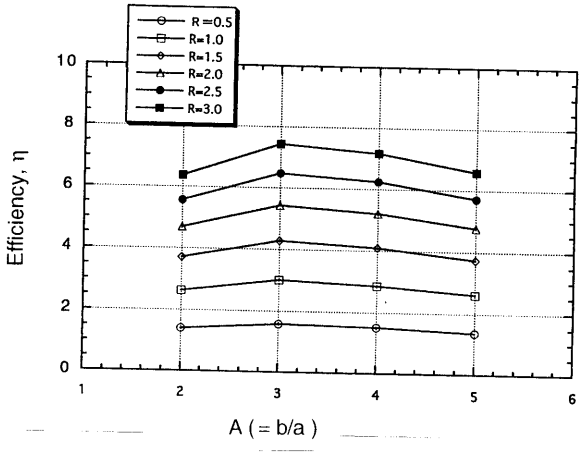

Fig. 13 Numerical results of η.

Conclusion

The MPD arcjet of which the electrodes are exposed to semi-infinite free space was analyzed to find the dimension of discharge region. The results are summarized as follows.

1) The discharge is mostly confined in the upstream. The result supports the design of EPEX/MPD arcjet as appropriate,
2) Since the discharge region is weakly influenced by the magnetic Reynolds number expressing the input power level, the dimension of MPD arcjet should be generally determined by the heat loading on the discharge chamber wall.

References

1) "Electric Propulsion Experiment (EPEX) of a Repetitively Pulsed MPD Thruster Syatem Onboard Space Flyer Unit (SFU)", IEPC-97-120, 25th IEPC, August 1997.

2) "Space Flyer Unit (SFU) Mission Report (Onboard Experiments)", ISAS Report Specia Edition, No.36, March, 1997.

3) Nishida E., Shimizu Y., and Kuriki, K., "Improved Thrust Generation Mechanism for Electrothermal /Electromagnetic Arcjet", IEPC-88-026, 20th IEPC, 1988.

4) Kunii Y., Shimizu Y. and Kuriki K., "Idealized Model for Plasma Acceleration in an MPD Channel", AIAA Journal, Vol. 21, No. 3, 1983.

5) Nakayama T., et.al., "Two Dimensional MPD", Journal of Propulsion and Power,

6) Itoh H., Master Thesis, Hokkaido Univ., 1993.

7) Jahn R. G., "Physics of Electric Propulsion", McGrow-Hill Press, 1968.